C. R. Physique 19 (2018) 553–560

Contents lists available at ScienceDirect

Comptes Rendus Physique

www.sciencedirect.com

Physics and arts / Physique et arts

X-ray diffraction and heterogeneous materials: An adaptive crystallography approach

Diffraction des rayons X et matériaux hétérogènes : une approche cristallographique adaptative

Catherine Dejoie [a,*], Pierre-Olivier Autran [a,b], Pierre Bordet [b], Andy N. Fitch [a], Pauline Martinetto [b], Philippe Sciau [c], Nobumichi Tamura [d], Jonathan Wright [a]

[a] *European Synchrotron Radiation Facility, Grenoble, France*
[b] *Université Grenoble Alpes, CNRS, Grenoble INP, Institut Néel, Grenoble, France*
[c] *CEMES, Toulouse, France*
[d] *Advanced Light Source, Lawrence Berkeley National Lab, Berkeley, USA*

ARTICLE INFO

Article history:
Available online 13 September 2018

Keywords:
Cultural heritage
Heterogeneous materials
X-ray diffraction
Crystalline phases
Amorphous phases
Synchrotron

Mots-clés :
Patrimoine culturel
Matériaux hétérogènes
Diffraction des rayons X
Phases cristallines
Phases amorphes
Synchrotron

ABSTRACT

Cultural heritage materials are often complex and heterogeneous, with a multi-scale architecture. Phases from a variety of crystalline forms co-exist in a wide grain size distribution, with each of these phases keeping in their structural arrangement a memory of the transformations that occurred to the material. Over the last two decades, X-ray diffraction has been applied successfully to the study of cultural heritage materials, with the use of synchrotron facilities offering new possibilities to describe the structural features of such complex materials. The long-range and/or short-range organization of the different crystallographic phases as well as their global position/dispersion in the material are closely related to the properties of the material (optical, mechanical...), its manufacturing process, functionality, or long-term conservation. In this paper, possible diffraction setups and data collection strategies are discussed in order to retrieve adequate data from crystalline and amorphous phases and to take into account single-crystal contributions.

RÉSUMÉ

Les matériaux du patrimoine sont souvent complexes et hétérogènes, avec une architecture multi-échelle. Plusieurs types de phases de cristallinité et de taille de grains variables coexistent, chacune d'entre elles préservant au sein de leur arrangement structural la mémoire des transformations ayant affecté le matériau au cours du temps. La diffraction des rayons X a été largement utilisée durant ces vingt dernières années pour étudier les matériaux du patrimoine, l'utilisation du rayonnement synchrotron offrant de nouvelles possibilités pour décrire leurs composantes structurales. Les propriétés de ces matériaux (optiques, mécaniques...), les étapes de leur élaboration, leur utilisation et leur conservation à long terme sont intimement liées à l'organisation à longue

* Corresponding author.
E-mail address: catherine.dejoie@esrf.fr (C. Dejoie).

https://doi.org/10.1016/j.crhy.2018.09.001

et courte distances des différentes phases cristallographiques qui les composent, ainsi qu'à leur position globale et/ou à leur dispersion. Dans cet article, plusieurs dispositifs expérimentaux et stratégies de collecte de données sont présentés, l'idée étant de pouvoir prendre en compte à la fois les phases cristallines (poudre et monocristaux) et amorphes.

1. Cultural heritage and X-ray diffraction

Cultural heritage materials have often complex and heterogeneous microstructure. Most of the time, they display a multi-scale architecture, composed by several phases and several crystalline forms. Some of these phases are well crystalline, but co-exist with less crystalline or amorphous ones. Crystal size may vary from one phase to the other, from a few nanometres to several tens of microns. The relative amount of each phase can also vary markedly, with the minority phases sometimes difficult to spot. Nevertheless, the properties of the material are intrinsically linked to the nature and the crystallographic structure of all these phases, the presence or the absence of interactions between them, and their global organization in the material. Ancient Jian ceramics (Song dynasty, 900–1200AC) are a good example of such complex architecture, from which remarkable properties emerge [1]. A dark-coloured body in which several crystalline phases co-exist is covered by a thick and mostly amorphous glaze. The silvery "oil spot" pattern that can be seen at the surface of the glaze of some of the most famous Jian wares originates from the precipitation of a two-dimensional dendritic network of the rare and metastable ε-Fe_2O_3 phase. This extraordinary patterning has elevated Jian ceramics to the rank of National Treasure in Japan. Deciphering the nature, the microstructure, and the interactions between the different phases of the material is the only way to understand the chemical and physical mechanisms at the origin of the ε-Fe_2O_3 phase formation and organization. If relevant from a cultural heritage point of view, such understanding may also provide new routes for the synthesis of ε-Fe_2O_3, a Fe_2O_3 polymorph showing unique magnetic properties [2].

The sequence of transformations that occurred to the material is imprinted in the atomic arrangement of its various crystallographic phases. Because of the presence of particular chemical elements or specific structural arrangements, some of these phases will give information on the provenance of the raw material used to craft the object, and so give insights into commercial routes and trade exchange behaviour in ancient time [3–5]. Others, by their presence, microstructure (crystallite size, strain) or arrangement in the material, will be related to the manufacturing process, e.g., the firing temperature and atmosphere for a ceramic [6], or the carburation process through repetitive hammering and heating of a nail [7] providing details on the know-how and everyday life of ancient civilizations. An additional aspect is the degradation or transformation over time and under specific conditions of some phases, resulting for example in the darkening of some pigments or formation of protrusions on paintings [8], offering new challenges for the preservation and conservation of the object for future generations. This long-term testing of the material, which cannot be re-produced easily in a laboratory, is also a unique opportunity to study the resistance of its components, and in so doing, design new, long-lasting materials for modern applications. The Maya Blue pigment, an organic–inorganic hybrid produced in Pre-Columbian Mesoamerica, is a perfect example of this archaeomimetic process [9], and has inspired numerous new hybrid materials [10–12].

X-ray diffraction methods are often chosen to perform advanced structural analyses, and, over the last two decades, they have been applied successfully to the study of cultural heritage materials. An illustrated summary of the information that can be obtained from diffraction data has been written by Artioli [13]. It is worth noting that, up to now, most of structural investigations in relation with cultural heritage has been carried out using the powder diffraction method. In a diffraction pattern, the positions of the diffraction peaks (or spots, in the case of single-crystal diffraction) are related to the symmetry of the crystal and the dimension of the unit cell, and their intensities to the nature and the positions of the atoms in the cell. An X-ray powder diffraction pattern is then like a fingerprint of the material, and can be used in a qualitative way for phase identification after comparison with a database. A more quantitative analysis through Rietveld refinement will provide the relative amount of each of the phases composing the material (see, for example, the study of a Roman fresco [14] or white pigments found in Grunewald paintings [15]). In the case of unknown compounds or incomplete structure (e.g., Maya Blue [16] and Catalan Blue pigments [17]), a complete crystal structure determination may be required. A shift of the peak positions compared to a reference can be related to the overall strain in the lattice of the crystal, and a given arrangement of the crystallites in the sample may affect intensities and produce a textured pattern [13,18]. In addition to position and intensity, the shape of a diffraction peak is a convolution between an instrumental contribution and microstructural effects coming from the sample. The broadening of a diffraction peak is then linked to the particle size of a given phase and/or some non-homogeneous strain in the lattice [19].

In addition to long-range ordering, a diffraction pattern also contains information about the local structure of the material. In particular, the contribution of the non-crystalline phases lies in the background of a powder pattern, and often is neglected. However, these phases may play an important role in the material as in the case of amorphous carbon-based pigments used in ink, painting or cosmetics during Roman time, and from which the dark colour is originating [20]. One of the challenges is to extract the diffraction signal of these amorphous phases among crystalline ones, and gain insight into their crystallographic structure. In order to obtain information about the short-to-medium range structural order of these

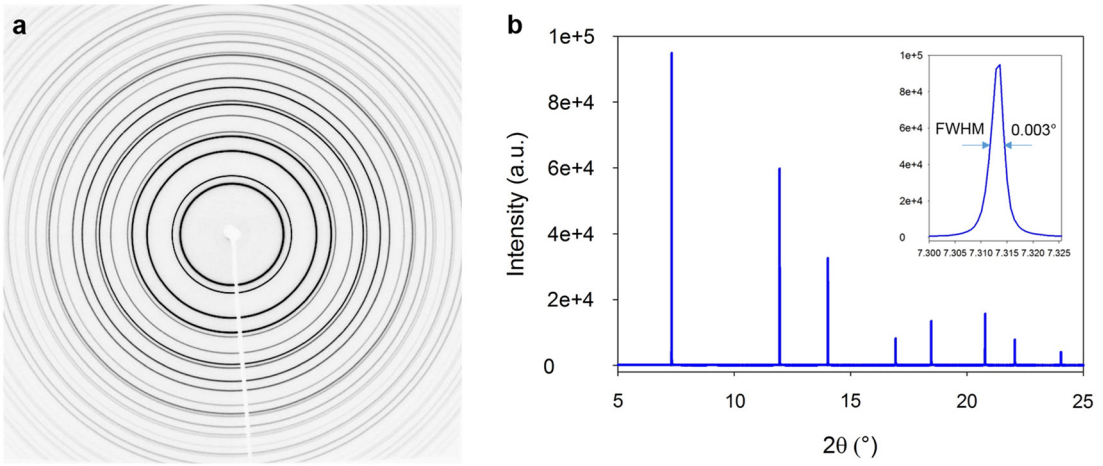

Fig. 1. a) Diffraction pattern of ceria measured with a FReLoN 4M 2D detector at the ID11 beamline (ESRF). b) High-resolution powder pattern of silicon (NIST, 640c) measured at the ID22 beamline (ESRF). The instrumental contribution to the full width at half maximum (FWHM) of diffraction peaks is about 0.003° 2θ (Si 111 reflection at 31 keV).

phases, pair distribution function analysis (PDF) can be used. Up to now, very few studies in relation with cultural heritage materials have been carried out using such analysis [21,22]. In the first section of the paper, possible strategies to retrieve high-quality data at a synchrotron facility for both Rietveld refinement and PDF analysis will be described.

Spatial resolution is achieved by decreasing the size of the incident X-ray beam, and today, micron to sub-micron beams can be obtained routinely at synchrotron facilities. The use of such a small beam is particularly interesting to perform 2D and 3D diffraction mappings of heterogeneous materials. In particular, 3D diffraction techniques such as X-ray diffraction computed-tomography [23] and computed X-ray laminography [24] have been successfully applied to the study of historical paintings [25,26]. Nevertheless, by decreasing the size of the incident beam and of the volume probed, the powder diffraction condition, which requires a large number of randomly oriented crystallites in the beam, may no longer be fulfilled. With a micron- or sub-micron-sized beam, only nanocrystalline phases will produce homogeneous powder diffraction rings. Phases made of larger crystallites will behave like single crystals, resulting in spotty diffraction rings and most of the time preventing any further (semi-)quantitative analysis. In order to take into account the single-crystal contribution while maintaining spatial resolution, an alternative to the powder diffraction method is desirable, and this will be discussed in the second section of the paper.

This paper is mainly focused on synchrotron X-ray diffraction and the study of heterogeneous materials. Some specific diffraction setups and technical aspects will be described, and alternative methods discussed. The data presented here were measured at three different synchrotron beamlines: the high-resolution powder diffraction beamline ID22 (formerly BM16 and ID31) and the materials science beamline ID11 at the European Synchrotron Radiation Facility (ESRF, Grenoble), and the microdiffraction beamline 12.3.2 at the Advanced Light Source (ALS, Berkeley).

2. X-ray powder diffraction and scattering, resolution and statistics

In an X-ray powder diffraction experiment, a monochromatic beam is scattered by the atoms of a sample, producing Debye–Scherer cones, the scattering angle of each cone being given by Bragg's law. The diffracted signal can be recorded through a flat plate detector (full or part of the diffraction rings will be visible) or by scanning a point detector through an arc that intercepts the Debye–Scherer cones, resulting in a one-dimensional powder pattern (Fig. 1). Both setups can be used for structural studies of heterogeneous materials, and some of the advantages and disadvantages in terms of peak shape, resolution, and statistics are discussed here.

The angular resolution of the diffraction peaks is an important factor in order to separate and identify the different phases of a sample and/or retrieve microstructural information from a peak-shape study. Several instrumental factors contribute to the width of a diffraction peak, such as the sample-detector distance, the divergence of the beam, some misalignment of the sample... The best resolution is achieved by placing an analyser crystal (e.g., a perfect Si 111 crystal) in the path of the diffracted beam before a point detector. A diffracted X-ray must strike the analyser crystal at precisely the correct Bragg angle to be diffracted into the detector. Since the acceptance of a Si 111 crystal is very small (a few arcsec), an analyser crystal stringently defines the 2θ angle of diffraction, yielding very narrow diffraction peaks. The efficiency of detecting the diffracted radiation can be increased by using several crystals in parallel [27], as done today at the high-resolution powder diffraction beamline ID22 [28]. The main drawbacks of the method are the scanning process that can be time consuming, and the loss in statistics due to the highly limited transmission of the diffracted beam by the analyser crystals. The use of a bidimensional (2D) detector to record the full diffraction rings would partially solve these problems, but at the detriment of resolution. Comparing the powder diffraction patterns obtained with a high-resolution

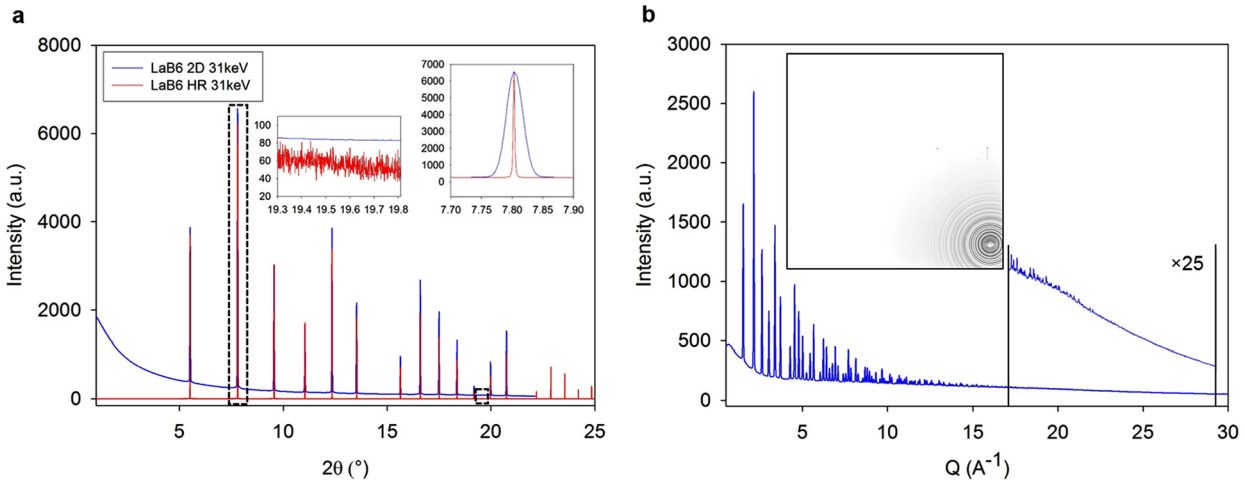

Fig. 2. a) Comparison between two powder diffraction patterns of LaB_6 (NIST, 660b) measured with the high-resolution setup (HR) and a flat panel PerkinElmer XRD 1611 detector (2D, 41 × 41 cm^2) at an energy of 31 keV. The intensity has been normalized using the 110 reflection (most intense peak, see inset). b) Powder diffraction pattern of LaB_6 measured for PDF analysis at an energy of 70 keV using the flat panel PerkinElmer detector. By integrating the 2D pattern along the diagonal, a Q_{max} of 29 $Å^{-1}$ is accessible.

setup and with a 2D detector is often complicated, as a lot of factors can be tuned to optimize both resolution and statistics (e.g., sample–detector distance, slit size, focusing of the incident beam...). The powder diffraction patterns of LaB6 (NIST standard 660b) obtained at ID22 at an energy of 31 keV (0.4 Å wavelength) using the high-resolution setup (scan speed of 2°/minute, average of 9 detectors) and from integration of a 2D pattern (average of 20 patterns, 50 ms per pattern) measured with a PerkinElmer XRD 1611 flat panel detector (41 × 41 cm^2, pixel size of 100 µm) are shown in Fig. 2a. The 2D detector was positioned at a distance of 1000 mm from the sample, which defines a 2θ range up to 22°, close to that of the high-resolution scan. A factor of 10 in peak-width resolution is obtained. On the other hand, the signal/noise ratio is clearly in favour of the pattern obtained using the 2D detector.

The possibility to have a good signal-to-noise ratio at high 2θ angle (or at high Q, $Q = 4\pi \sin(\theta)/\lambda$) is particularly crucial in order to perform good quality PDF analyses. Indeed, the experimental PDF $G(r)$ is obtained by Fourier transform of the normalized total structure factor $S(Q)$, derived from a powder diffraction pattern corrected from various factors (sample environment, incoherent scattering ...). High-Q data are necessary to limit Fourier termination errors, but may suffer from a lack of statistics due to the decrease of the X-ray scattering power. The highest Q that can be achieved with a given setup is defined by the maximum 2θ angle that can be reached as well as the energy of the incident beam. For example, a Q of 29 $Å^{-1}$ can be obtained on ID22 from powder data collected at an energy of 70 keV with a large 2D PerkinElmer detector positioned at 380 mm from the sample (Fig. 2b). The use of a 2D detector ensures high counting statistics, especially at high angles, and a pattern adequate for PDF analysis can be collected in a few minutes (from 5 to 30 min, depending on the sample). Nevertheless, in the case of crystalline or semi-crystalline samples, data for both Rietveld and pair distribution function analyses may be required, and in that case, a high-resolution setup could be desirable. At the ID22 beamline and for an energy of 31 keV, a high-resolution pattern with sufficient statistics up to 140° 2θ ($Q_{max} = 30$ $Å^{-1}$) can take 2 to 3 h.

The best compromise would be to combine in the same setup high resolution provided by analyser crystals with high efficiency provided by a 2D detector. Such a possibility has been recently tested on ID22, when the nine-scintillator detectors positioned behind the nine analyser crystals were replaced by a 2D Pilatus3 X CdTe 300K-W detector, large enough to cover the nine diffraction zones. During a 2θ scan, at each nominal 2θ value, a 2D image is recorded, and nine distinct regions of the 2D image correspond to the diffraction signals passing via each of the analyser crystals. The possibility to observe the 2D diffraction signal obtained at each point of a 2θ scan behind an analyser crystal gives important indications that can be used to improve the quality of high-resolution powder diffraction patterns. For instance, the axial (horizontal) acceptance, usually defined by a fixed receiving aperture placed in front of the nine detectors, plays an important role in the quality of the data. At low diffraction angle, because of the curvature of the Debye–Scherrer cones, a too large axial acceptance results in broadened and asymmetric peaks. On the other hand, at high diffraction angles, detection efficiency can be improved by up to an order of magnitude by increasing axial acceptance. By simply choosing the appropriate region to integrate on the 2D images collected with the 2D detector, the effective axial aperture can be varied as a function of 2θ (Fig. 3), narrow at low angle where the curvature of the Debye–Scherrer cones is most marked, and wider at higher angle, where the curvature is less, resulting in an optimization of both peak shape and statistics, and consequently decreasing the data collection time without sacrificing angular resolution. An additional benefit of having access to the 2D images in the case of heterogeneous samples is the possibility to monitor the diffraction contributions of both powder phases and single-crystal phases. Diffraction spots from large grains are usually much stronger than the average signal seen per pixel and originating

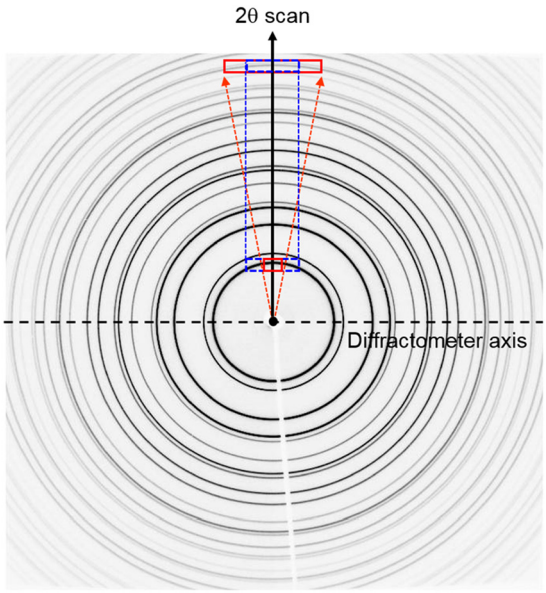

Fig. 3. Reproduced from reference [29]. Schematic representation of the accessible diffraction domain in order to retrieve a high-resolution powder pattern. In the ordinary setup available at ID22, a 4-mm fixed axial aperture is scanned along 2θ intercepting the Debye–Scherrer rings (blue dashed window). In an optimal setup, the aperture should be varied as a function of 2θ, narrow at low angle to avoid the asymmetry effect and wider at higher angle to improve statistics (red window). The use of a 2D detector behind the analyser crystals would allow such data handling flexibility.

from small crystallites, and might therefore be removed by suitable filtering. In such a way, usable powder intensities are retrieved, and better-quality Rietveld refinement can be performed [29].

3. White or pink, changing the colour of the beam

When only one (or a few) crystal(s) are exposed to an X-ray beam, discrete diffraction spots are produced and can be recorded on an area detector. A classic single-crystal diffraction experiment requires the rotation of a crystal in a monochromatic beam in order to measure enough reflections and retrieve full intensities. Employing a monochromatic beam to retrieve structural information from a single crystal becomes more challenging when the sample cannot be fully rotated and for crystals embedded in a complex matrix. In such a case, the Laue method may be more appropriate. The sample is exposed to a broad energy band-pass (polychromatic or white beam) (Fig. 4a), and a large number of reflections can be recorded simultaneously in a single exposure on a 2D detector. The potential of the Laue method has been exploited in the 1980s by the protein community [30], and later on, it has been applied to materials science [31,32]. In the latter case, a single diffraction pattern is usually enough to retrieve the orientation of the crystal, to acquire information about possible distortion, and, after adequate corrections, to extract usable intensities. If structure solution and refinement require a few frames with random orientations to be combined to obtain sufficient completeness [33], semi-quantitative analysis can be performed simply after indexing a single Laue pattern (which means attributing to each reflection its corresponding *hkl* and retrieving the orientation matrix). This is the reason why the Laue method is applied today to the mapping of grain orientation and crystal distortion in polycrystalline and composite materials with a spatial resolution of a micron (or less) [34,35]. The Laue microdiffraction technique has been applied in the investigation of a few materials in relation with cultural heritage, such as the Chinese purple pigment used in the decoration of terracotta warriors from the Qin dynasty [36], or pigments from an Egyptian coffin [37].

In the case of materials showing a strong heterogeneity at different length scales (from a few tens of microns to a few tens of nanometres), one of the main interests is to combine Laue single-crystal diffraction with monochromatic powder diffraction. Above all, by mapping the same zone of the sample with a micron-sized beam, and simply switching from monochromatic to Laue mode, both the microcrystalline and the nanocrystalline part of the material can be investigated. The main constraint is to keep the beam at the same position on the sample when changing the diffraction mode. This can be done at a few beamlines around the world, such as BL12.3.2 at the ALS, where a four-bounce monochromator can be inserted or removed quickly while accurately maintaining the beam position on the sample. As an example, such a mapping procedure has been applied to Neolithic flints, where both nanocrystalline quartz and large crystals of detritic quartz co-exist [7]. If the coherent domain size of nanocrystalline quartz is not affected by moderate heating, this is sufficient for observing residual strain relaxation from large crystals. This gives information about the practical knowledge of Neolithic societies, evidencing a slow and controlled fabrication process of flints. This possibility of switching between two diffraction modes is also interesting for *in situ* experiments, when the grain size of the sample evolves with pressure or temperature. To illustrate the complementarity between both diffraction modes, the diffraction patterns obtained using a monochromatic

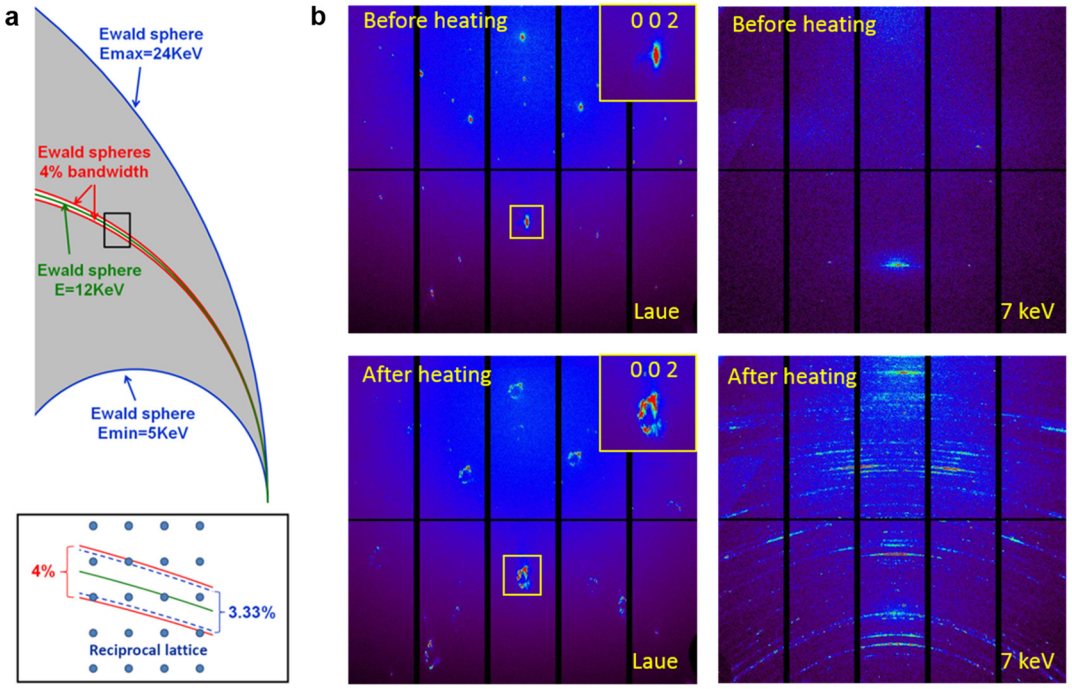

Fig. 4. a) Reproduced from reference [39]. Ewald construction for Laue mode as available at the beamline 12.3.2 at ALS (5–24 keV), monochromatic mode (12 keV) and 4% bandwidth 'extra pink' beam mode. The inset shows that if more reflections are in condition of diffraction, the partial reflection intensity problem inherent to monochromatic diffraction (in a single image, only part of the diffraction nodes are intercepted) can also be overcome when using a non-monochromatic beam (using a 4% bandpass beam, reflections within 3.33% bandpass will be fully measured, leading to correct intensities). b) Two diffraction patterns recorded on a large galena single crystal using both white beam (5–24 keV) and monochromatic beam (7 keV) before and after heating at 500 °C.

beam (7 keV) and a Laue beam (5–24 keV range) on a large galena (PbS) crystal before and after heating are shown on Fig. 4b. Galena has been used as black pigment for the formulation of cosmetics during Antiquity. Different shades of galena-based eye make-up may be obtained after thermal treatment, in relation with the formation of an oxide layer at the surface of PbS crystals. Before the heating process, only a few large diffraction spots can be seen on the pattern taken with a monochromatic beam, in accordance with the presence of a large single crystal in the beam. On the other hand, the pattern recorded in Laue mode shows nice diffraction spots and can be indexed using galena structural parameters. After heating the crystal at 500 °C, an oxidized layer made of small crystals of anglesite ($PbSO_4$) appears at the surface, and the corresponding diffraction rings can be seen in the powder pattern. The underlying galena crystal has also evolved, the Laue spots being now strongly distorted.

If the possibility of fast switching between Laue and monochromatic modes is an efficient way to look at heterogeneous materials, the sample still needs to be mapped twice to get both single-crystal and powder information. The best would be to retrieve complementary information in a single scan while keeping adequate spatial resolution. To do so, the use of a "pink" beam (bandpass $\Delta E/E \approx 1$–4%, e.g., an energy range of a few tens/hundreds of eV), intermediate between a strictly monochromatic beam ($\Delta E/E \approx 10^{-4}$) and a white beam (energy range 5–24 keV) could be an attractive solution. With such a beam, the resolution of the powder diffraction peaks will decrease, but the main part of the diffraction signal should be preserved. Concerning the single-crystal part, more nodes of the reciprocal lattice will satisfy the diffraction condition, making the indexing of a single image and intensity extraction easier (Fig. 4a). The interest of using broad-bandpass diffraction for serial crystallography has already been demonstrated, as such a diffraction mode will be available at the new X-ray free-electron laser source (SwissFEL) in Switzerland [38], and data processing tools are already available [39]. In order to look at the effect of such a beam on the powder part of the sample, a test has been carried out at the materials science beamline ID11 at ESRF, which is equipped with an *in vacuum* transfocator that allows a broad-bandpass mode of about 1.5% [40]. Diffraction data have been measured on a Ni sample using a 2-μm beam at an energy close to 65.3 keV. A powder pattern was retrieved, and Fourier transformed for PDF analysis. These data have been compared with that obtained on the same sample with a monochromatic beam (Fig. 5). If the width of diffraction peaks does not show significant difference at low angle, a progressive loss in resolution with increasing angles is observed. This affects the damping of the PDF in real space, making the large-*r* region more difficult to interpret. Nevertheless, good-quality Rietveld and PDF refinements could be obtained. It is worth mentioning that a factor of 5 in intensity was gained with the pink-beam setup. This demonstrates that the use of a pink-beam mode may be an interesting alternative to perform 2D or 3D mapping of heterogeneous samples, with the possibility of obtaining simultaneously powder and single-crystal data, while increasing the overall intensity.

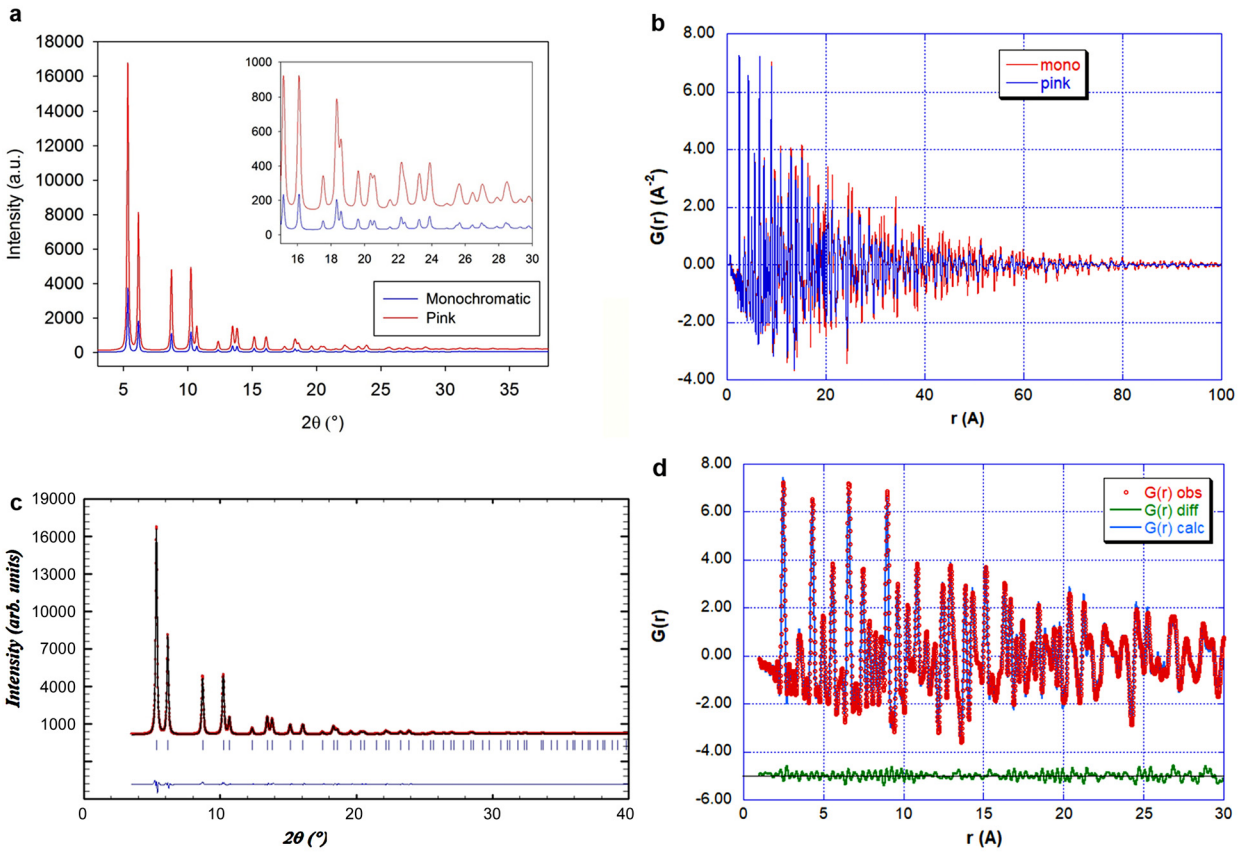

Fig. 5. a) Comparison between the powder diffraction patterns of nickel obtained using a monochromatic beam (65.3 keV) and a pink beam (1.5% bandpass around 65.3 keV) at the ID11 beamline (ESRF). Although resolution at high angle has decreased, a factor 5 in intensity is obtained. b) Corresponding PDFs, showing a faster damping for the one retrieved from the pink-beam pattern. c) Rietveld refinement and d) PDF refinement of the powder pattern obtained using pink beam.

4. Conclusion

In order to decipher the intimate structure of heterogeneous materials, a single diffraction method is often not enough. By adapting the experimental setup and the data collection strategy, by taking advantage of the flexibility of a synchrotron beamline, several diffraction methods can be combined, and new strategies may emerge. This is always a back-and-forth process, the complexity of the material calling for new adapted methods, and the use of advanced method being required to understand all the aspects of the material. The importance of developing adapted computing tools to facilitate data handling and processing should also be mentioned. Cultural heritage materials, because of their intrinsic heterogeneity, moreover because they are sometimes unique, are usually good candidates for pushing towards special developments, which can be of benefit to other areas of materials science.

Acknowledgements

The ID22 beamline at ESRF was kindly provided with a Pilatus3 X CdTe 300K-W detector by Dectris. The authors thank Carlotta Giacobbe (ESRF Grenoble) for kindly helping processing some of the figures, as well as the staffs of the ID22, ID11 and BL12.3.2 beamlines for their support and fruitful discussions. The Advanced Light Source at the Lawrence Berkeley National Laboratory is supported by the Office of Science, Office of Basic Energy Sciences, Scientific User Facilities Division of the U.S. Department of Energy under Contract No. DE-AC02-05CH11231.

References

[1] C. Dejoie, P. Sciau, W. Li, L. Noé, A. Mehta, K. Chen, H. Luo, M. Kunz, N. Tamura, Z. Liu, Learning from the past: Rare ε-Fe_2O_3 in the ancient black-glazed Jian (Tenmoku) wares, Sci. Rep. 4 (4941) (2014) 1–8.

[2] M. Gich, C. Frontera, A. Roig, J. Fontcuberta, E. Molins, N. Bellido, C. Simon, C. Fleta, Magnetoelectric coupling in ε-Fe_2O_3 nanoparticles, Nanotechnology 17 (2006) 687–691.

[3] T. Calligaro, A. Mossmann, J.-P. Poirot, G. Querré, Provenance study of rubies from a Parthian statuette by PIXE analysis, Nucl. Instr. Meth. Phys. Res. B 136–138 (1998) 846–850.
[4] M. Filomena Guerra, T. Calligaro, Gold cultural heritage objects: a review of studies of provenance and manufacturing technologies, Meas. Sci. Technol. 14 (2003) 1527–1537.
[5] L. Bellot-Gurlet, G. Poupeau, J. Salomon, T. Calligaro, B. Moignard, J.C. Dran, J.A. Barrat, L. Pichon, Obsidian provenance studies in archaeology: a comparison between PIXE, ICP-AES and ICP-MS, Nucl. Instr. Meth. Phys. Res. B 240 (2005) 583–588.
[6] P. Sciau, S. Relaix, C. Roucau, Y. Kihn, D. Chabanne, Microstructural and microchemical characterization of roman period terra sigillate slips from archeological sites in southern France, J. Am. Ceram. Soc. 89 (2006) 1053–1058.
[7] C. Dejoie, N. Tamura, M. Kunz, P. Goudeau, P. Sciau, Complementary use of monochromatic and white-beam X-ray micro-diffraction for the investigation of ancient materials, J. Appl. Crystallogr. 48 (2015) 1522–1533.
[8] M. Cotte, E. Checroun, W. De Nolf, Y. Taniguchi, L. De Viguerie, M. Burghammer, P. Walter, C. Rivard, M. Salomé, K. Janssens, J. Susini, Lead soaps in paintings: friends or foes?, Stud. Conserv. 62 (2017) 2–23.
[9] P. Gómez-Romero, C. Sánchez, Hybrid materials. Functional properties. From Maya Blue to 21st century materials, New J. Chem. 29 (2005) 57–58.
[10] C. Dejoie, P. Martinetto, N. Tamura, M. Kunz, F. Porcher, P. Bordat, R. Brown, E. Dooryhée, M. Anne, L.B. McCusker, Crystal structure of an indigo@ silicalite hybrid related to the ancient Maya blue pigment, J. Phys. Chem. C 118 (2014) 28032–28042.
[11] E. Lima, P. Bosch, S. Loera, I.A. Ibarra, H. Laguna, V. Lara, Non toxic hybrid pigments: sequestering betanidin chromophores on inorganic matrices, Appl. Clay Sci. 42 (2009) 478–482.
[12] X. Zhang, Z. Jin, Y. Li, S. Li, G. Lu, Photosensitized reduction of water to hydrogen using novel Maya blue-like organic–inorganic hybrid material, J. Colloid Interface Sci. 333 (2008) 285–293.
[13] G. Artioli, Science for the cultural heritage: the contribution of X-ray diffraction, Rend. Lincei, Sci. Fis. Nat. 24 (2013) 55–62.
[14] E. Dooryhee, M. Anne, I. Bardies, J.L. Hodeau, P. Martinetto, S. Rondot, J. Salomon, G.B.M. Vaughan, P. Walter, Non-destructive synchrotron X-ray diffraction mapping of a Roman painting, Appl. Phys. A 81 (2005) 663–667.
[15] E. Welcomme, P. Walter, P. Bleuet, J.-L. Hodeau, E. Dooryhee, P. Martinetto, M. Menu, Classification of lead white pigments using synchrotron radiation micro X-ray diffraction, Appl. Phys. A 89 (2007) 825–832.
[16] G. Chiari, R. Giustetto, G. Ricchiardi, Crystal structure refinements of palygorskite and Maya Blue from molecular modelling and powder synchrotron diffraction, Eur. J. Mineral. 15 (2003) 21–33.
[17] J. Rius, E. Elkaim, X. Torrelles, Structure determination of the blue mineral pigment aerinite from synchrotron powder diffraction data: the solution of an old riddle, Eur. J. Mineral. 16 (2004) 127–134.
[18] I. Lonardelli, H.R. Wenk, L. Lutterotti, M. Goodwin, Texture analysis from synchrotron diffraction images with the Rietveld method: dinosaur tendon and salmon scale, J. Synchrotron Radiat. 12 (2005) 354–360.
[19] T. Ungar, P. Martinetto, G. Ribarik, E. Dooryhee, P. Walter, M. Anne, Revealing the powdering methods of black makeup in Ancient Egypt by fitting microstructure-based Fourier coefficients to the whole X-ray diffraction profiles of galena, J. Appl. Phys. 91 (2002) 2455–2465.
[20] M.C. Gamberini, C. Baraldi, F. Palazzoli, E. Ribechini, P. Baraldi, MicroRaman and infrared spectroscopic characterization of ancient cosmetics, Vib. Spectrosc. 47 (2008) 82–90.
[21] L. Samain, F. Grandjean, G.J. Long, P. Martinetto, P. Bordet, D. Strivay, Relationship between the synthesis of Prussian blue pigments, their color, physical properties, and their behavior in paint layers, J. Phys. Chem. C 117 (2013) 9693–9712.
[22] S. Cersoy, P. Martinetto, P. Bordet, J.-L. Hodeau, E. Van Elslande, P. Walter, Identifying and quantifying amorphous and crystalline content in complex powdered samples: application to archaeological carbon blacks, J. Appl. Crystallogr. 49 (2016) 585–593.
[23] P. Bleuet, E. Welcomme, E. Dooryhee, J. Susini, J.-L. Hodeau, P. Walter, Probing the structure of heterogeneous diluted materials by diffraction tomography, Nat. Mater. 7 (2008) 468–472.
[24] S. Legrand, F. Vanmeert, G. van der Snickt, M. Alfeld, W. de Nolf, J. Dik, K. Janssens, Examination of historical paintings by state-of-the-art hyperspectral imaging methods: from scanning infra-red spectroscopy to computed X-ray laminography, Herit. Sci. 2 (2014) 1–11.
[25] W. de Nolf, K. Janssens, Micro X-ray diffraction and fluorescence tomography for the study of multilayered automotive paints, Surf. Interface Anal. 42 (2010) 411–418.
[26] F. Vanmeert, G. van der Snickt, K. Janssens, Plumbonacrite identified by X-ray powder diffraction tomography as a missing link during degradation of red lead in a Van Gogh painting, Angew. Chem. 127 (2015) 3678–3681.
[27] J.-L. Hodeau, P. Bordet, M. Anne, A. Prat, A.N. Fitch, E. Dooryhée, G. Vaughan, A. Freund, Nine-crystal multianalyzer stage for high-resolution powder diffraction between 6 keV and 40 keV, Proc. SPIE 3448 (1998) 353–361.
[28] A.N. Fitch, The high resolution powder diffraction beam line at ESRF, J. Res. Natl. Inst. Stand. Technol. 109 (2004) 133–142.
[29] C. Dejoie, M. Coduri, C. Giacobbe, P.O. Autran, M.W. Mogodi, E. Covacci, O. Grimaldi, S. Petitdemange, D. Sisak-Jung, A.N. Fitch, Combining a nine-crystal multi-analyzer stage with a 2-dimensional detector for high-resolution powder X-ray diffraction, J. Appl. Crystallogr. (2018), submitted for publication.
[30] J.R. Helliwell, Synchrotron X-radiation protein crystallography: instrumentation, methods and applications, Rep. Prog. Phys. 47 (1984) 1403–1497.
[31] N. Tamura, A.A. MacDowell, R. Spolenak, B.C. Valek, J.C. Bravman, W.L. Brown, R.S. Celestre, H.A. Padmore, B.W. Batterman, J.R. Patel, Scanning X-ray microdiffraction with submicrometer white beam for strain/stress and orientation mapping in thin films, J. Synchrotron Radiat. 10 (2003) 137–143.
[32] X. Chen, C. Dejoie, T. Jiang, C.S. Ku, N. Tamura, Quantitative microstructural imaging by scanning Laue X-ray micro-and nanodiffraction, Mater. Res. Soc. Bull. 41 (2016) 445–453.
[33] C. Dejoie, L.B. McCusker, C. Baerlocher, M. Kunz, N. Tamura, Can Laue microdiffraction be used to solve and refine complex inorganic structures?, J. Appl. Crystallogr. 46 (2013) 1805–1816.
[34] M. Kunz, K. Chen, N. Tamura, H.R. Wenk, Evidence for residual elastic strain in deformed natural quartz, Am. Mineral. 94 (2009) 1059–1062.
[35] K. Chen, C. Dejoie, H.R. Wenk, Unambiguous indexing of trigonal crystals from white-beam Laue diffraction patterns: application to Dauphiné twinning and lattice stress mapping in deformed quartz, J. Appl. Crystallogr. 45 (2012) 982–989.
[36] Z. Liu, A. Mehta, N. Tamura, D. Pickard, B. Rong, T. Zhou, P. Pianetta, Influence of Taoism on the invention of the purple pigment used on the Qin terracotta warriors, J. Archaeol. Sci. 34 (2007) 1878–1883.
[37] P.A. Lynch, N. Tamura, D. Lau, I. Madsen, D. Liang, M. Strohschnieder, A.W. Stevenson, Application of white-beam X-ray microdiffraction for the study of mineralogical phase identification in ancient Egyptian pigments, J. Appl. Crystallogr. 40 (2007) 1089–1096.
[38] B.D. Patterson, P. Beaud, H.H. Braun, C. Dejoie, G. Ingold, C. Milne, L. Patthey, B. Pedrini, J. Szlachentko, R.l Abela, Science opportunities at the SwissFEL X-ray laser, Chimia 68 (2014) 73–78.
[39] C. Dejoie, L.B. McCusker, C. Baerlocher, R. Abela, B.D. Patterson, M. Kunz, N. Tamura, Using a non-monochromatic microbeam for serial snapshot crystallography, J. Appl. Crystallogr. 46 (2013) 791–794.
[40] G.B.M. Vaughan, J.P. Wright, A. Bytchkov, M. Rossat, H. Gleyzolle, I. Snigireva, A. Snigirev, X-ray transfocators: focusing devices based on compound refractive lenses, J. Synchrotron Radiat. 18 (2011) 125–133.